Presented at the 32nd European PV Solar Energy Conference and Exhibition, 20-24 June 2016, Munich, Germany

OPTIMIZED GRAIN SIZE OF SEED PLATES FOR HIGH PERFORMANCE MULTICRYSTALLINE SILICON

Patricia Krenckel, Stephan Riepe, Florian Schindler, Theresa Strauch
Fraunhofer Institute for Solar Energy Systems ISE
Heidenhofstrasse 2, D-79110 Freiburg, Germany

ABSTRACT: Two silicon ingots with different seed plate configurations were crystallized by directional solidification. Seed plates with high performance multicrystalline structure varying in their mean grain area were used as well as seed plates with comparable mean grain area varying in their grain structure (standard and high performance multicrystalline). All grown materials show an increase of grain size and saturation at different levels with ingot height. Additionally, a dependence of the growth behavior on the mean grain area was observed implying a faster coarsening for smaller grains. The material grown on the standard multicrystalline seed plate shows a larger area fraction limited by dislocations than the material with high performance multicrystalline seed plates, showing less dislocation structures on samples with smaller grains. The minority carrier lifetimes measured on passivated samples after a boron diffusion, as used in high efficiency solar cell processes for n-type silicon, showed a benefit for the material grown on a high performance multicrystalline seed plate with smaller grains compared to the other materials. The harmonic mean lifetime values are even higher than corresponding ones for high performance multicrystalline material nucleated on granular beads. The same trend was seen in ELBA, a combination of injection-dependent lifetime measurements on processed samples with PC1D simulations, which estimates material-related efficiency losses of only 0.4 % compared with the solar cell limit of an n-type solar cell structure on material nucleated on the fine grained seed plate with high performance multicrystalline structure.

Keywords: Crystallization, Seeded growth, Defects, Multicrystalline Silicon

1 INTRODUCTION

Currently, the solar cell market is dominated by the so-called high performance multicrystalline silicon (HPM), which holds a market share of about 40 % in 2015 and will replace the share of standard multicrystalline silicon completely [1]. The homogeneous and randomly oriented grain structure of HPM silicon reduces the evolution of dislocation clusters due to the overgrowth of dislocated grains [2]. One method for the production of HPM silicon is the use of seed materials, especially granular silicon beads [3], another one is the nucleation at the crucible coating. Both lead to the typically uniform grain size distribution at the ingot bottom.

HPM silicon as established in the industry reaches average solar cell efficiencies in the range of 19 %. The low dislocation densities result from the homogeneous, fine grain structure [4]. Due to the fact that dislocations are no longer the efficiency limiting factor in most parts of these ingots, the fraction of grain boundaries should be reduced to increase the material quality for higher solar cell efficiencies. However, an increase of the mean grain area even with sustained homogeneity of the grain structure could lead to higher dislocation densities and clusters, which would again limit the efficiency. Thus, the understanding of the trade-off between the amount of grain boundaries and dislocations is essential to find an optimum grain structure for high efficiency solar cells.

Previous experiments have shown that the same low dislocation density can be obtained for the use of small seed crystals as well as for the use of seed plates with the typical HPM grain structure, which allow a grain size variation [5]. For HPM silicon ingots produced with seeded growth on small sized silicon material, the properties of the seed material determine the initial grain structure and sizes of the crystallites at the bottom of the ingot. A variation of the mean grain area or their distributionin the initial grain structure of the ingot is possible by the use of seed plates with a pre-defined grain structure. The comparison of two different seed materials in one crystallization experiment generates wafers of comparable impurity concentrations, only varying in their grain structure. This procedure allows an evaluation of the optimum seed configuration for highly efficient solar cells.

This work aims for the development of HPM silicon ingots with continuously low dislocation densities and optimized grain structure based on the use of seed plates. Two ingots with different kinds of seed plates, varying in structure and mean grain area, were crystallized. Calculating solar cell efficiency potentials via ELBA analyses [6; 7], an optimized seed plate configuration is estimated.

2 EXPERIMENTAL PROCEDURE

2.1 Seed configuration

The seed materials for the ingots described in the following section were different silicon plates with a thickness of 30 mm. The seed plates were cut from previously crystallized ingots at Fraunhofer ISE. For each of the two crystallized ingots, four different seed configurations were used but only two of them are discussed in this work.

The first ingot was crystallized with two seed plates with comparable mean grain area varying in their grain distribution and homogeneity. One seed plate was taken from a previously crystallized HPM ingot. The second seed plate features a standard multicrystalline structure with the same mean grain area. These parts are labeled “HPM medium” and “mc medium” in the following.

For the second ingot, two seed plates from different brick heights from the HPM grown ingot used for the first ingot in this work were used. Due to their different height positions in the previously crystallized ingot, they are comparable in structure but vary in grain size. One

finely grained seed plate was cut from the bottom part, and one larger grained from the top part. The crystallized parts from these seeds are labeled “HPM small” and “HPM large” in the following.

2.2 Directional solidification

Two n-type multicrystalline silicon ingots of G2 size, equivalent to 75 kg silicon and an ingot height of 220 mm, have been crystallized by directional solidification. For both ingots, pre-coated industrial quartz crucibles were used. The seed arrangement explained in the previous section was placed at the crucible bottom and covered with high purity silicon feedstock. Both ingots were charged with highly phosphorous doped monocrystalline silicon chunks to achieve a resistivity of approximately 1 Ωcm. For both crystallizations, the same thermal process including the heating up, melting from sides and top, crystallization from bottom to top and cooling down was used. For the main growth process after the nucleation phase, a growth velocity of 8 mm/h was achieved.

2.3. Material analysis

A centered brick of the size of 156 x 156 mm^2 was cut from each ingot. After polishing of the brick sides and a bottom and top cut off, the bricks were wafered with a wafer thickness of 210 µm. Automated photoluminescence measurements were performed on all “as cut” wafers. The grain structure was depicted by optical analyses of the wafer surface. Image analysis provides different structural parameters as mean grain area, weighted percentiles of grain areas, cumulative length of all grain boundaries, and the aspect ratio of the grain shape [8].

Selected wafers from four different heights of the second ingot were reduced to 125 x 125 mm^2 for further processing. From each height, one wafer was boron diffused as used for emitter formation in an n-type high efficiency solar cell process [9]. For the preparation of lifetime samples, the diffused layers were etched back and all selected wafers received a silicon nitride passivation layer on both sides. These wafers were used for spatially resolved lifetime measurements with a calibration via quasi-steady-state photoluminescence [10]. The minority carrier lifetime was harmonically averaged on specific areas. Further analysis of the efficiency limiting bulk recombination, so called ELBA, was applied [6; 7]. The combination of injection-dependent lifetime measurements on these processed samples with PC1D simulations of the TOPCon cell concept gives indications of the efficiency potentials of solar cells on this material [11]. The parameters used in the PC1D simulations are taken from [9] (cell limit without bulk recombination and with isotextured boron-diffused front side: 20.9 %).

All shown material analyses were evaluated for the wafer parts corresponding to the different seed configurations separately.

3 RESULTS

3.1 Grain structure

As a first and most common parameter, the mean grain area was calculated for the different seed configurations over ingot height, see Figure 1. All examined configurations show a growing mean grain area over ingot height, so called coarsening of grains. The seed plate with the smallest grain size, HPM small, starts at smaller grain sizes, both other HPM seeds at a comparable grain size. At an ingot height between 130 mm and 150 mm, saturation of the mean grain size value is visible for all materials.

As an alternative parameter, the weighted median indicating a grain size at which all smaller grains account for one half of the wafer area and all larger grains for the other half is less affected by small grains [8]. For the HPM seeded material, both parameters show the same trend, which illustrates the homogeneity of the grain structure. Only the multicrystalline seed leads to a larger variation in grain size distribution.

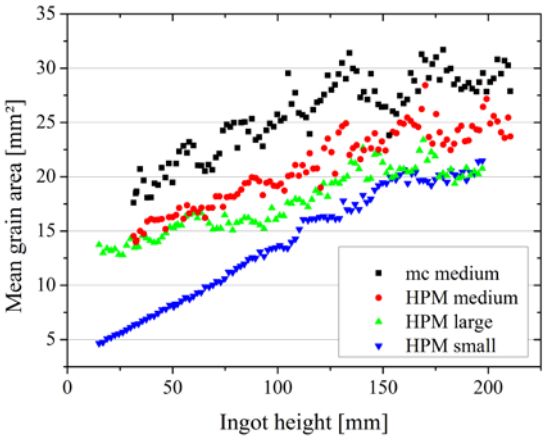

Figure 1: Mean grain area of all different seed configurations over ingot height.

The consideration of the height profiles of the percentiles 30 and 70, indicating the grain size at which all smaller grains account for 30 % respectively 70 % of the wafer area, depicts the coarsening of grains up to an ingot height of approx. 150 mm, see Figure 2. Starting from that ingot height, the grain structure of both materials seems to be very similar for the upper part. The other percentiles show the same behavior over ingot height. Additionally, a dependence of the coarsening on the mean grain size is visible. The smallest HPM seed plate induces a stronger coarsening at the beginning than all other seed plates, which show a comparable coarsening.

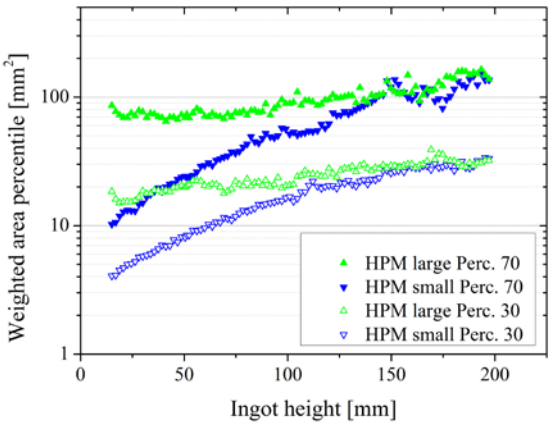

Figure 2: Weighted area percentiles 30 and 70 for the seed configurations HPM small and HPM large.

The cumulated grain boundary length normed on the considered wafer area decreases with ingot height correlating with increasing grain sizes. The smallest seed configuration leads to the fastest coarsening and thus the strongest reduction of grain boundaries. The HPM seeds show a comparable amount of grain boundaries at the ingot top, whereas the mc seed has a constantly lower grain boundary length due to some very large grains.

Besides the size of grains, the shape is an important parameter due to its correlation with grain boundaries. The aspect ratio is calculated by the ratio of minor and major axis of an ellipse fitted on each grain, giving a value between zero and one. The mean aspect ratio for the HPM seeds decreases with ingot height whereas it increases for the mc seed, see Figure 3. HPM material starts with homogeneous, round grains enlarging and narrowing to ingot top, whereas grains in mc material are inhomogeneous and irregular. For grains with an aspect ratio smaller than 0.25 a good correlation with twin grains is given [8]. With this optical identification, a higher share of twinned grains for the mc seed (more than 30 % of the relevant wafer area) than HPM seeds (between 10 % and 20 % of the relevant wafer area), is found. The increase of the mean aspect ratio of the mc seed for the second half of the ingot is correlated to a decrease in the area share of twinned grains.

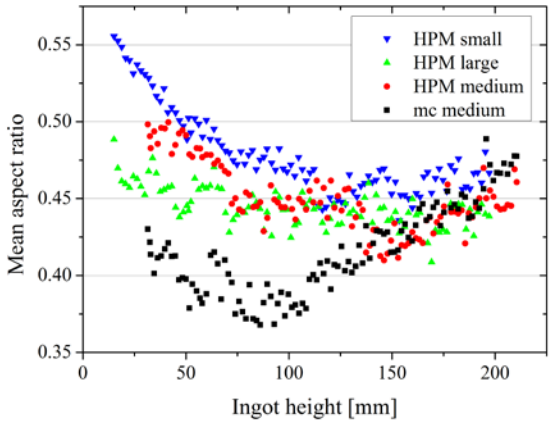

Figure 3: Height profile of the mean aspect ratio for all seed plates.

3.2 PL images and dislocations

The spatial resolution of recombination active structures such as grain boundaries and dislocations can be seen in photoluminescence (PL) images indicated by darker regions. The main percentage of the recombination in the ingot middle can be ascribed to grain boundaries for all different seed configurations, see Figure 4. Of course, the larger the grains are the smaller is the area share of the grain boundaries and thus the recombination induced by them. The area fraction of dislocated material is the largest for the mc medium seed. It is comparably low for all investigated HPM seeds, even though it seems a bit smaller for the investigated wafers from larger HPM seeds.

Considering the evolution over the whole ingot height, the area affected by dislocations is higher for the ingot bottom and top. Dislocations outlast longer and multiply very fast in large grains in the mc seed region. In comparison, the area affected by dislocations is smaller for bottom and top for HPM seed plates. In the bottom and top region, more dislocations are visible in both HPM samples with larger grains, HPM large and HPM medium.

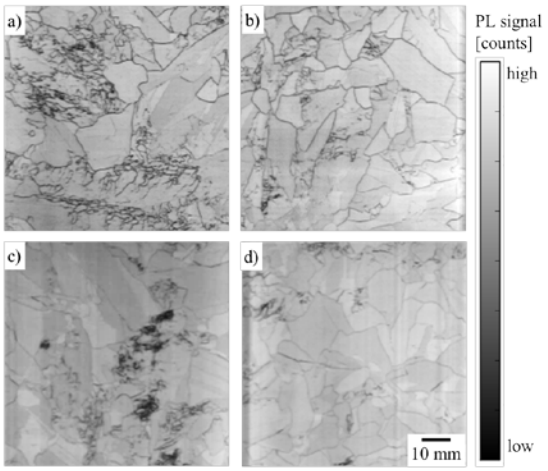

Figure 4: PL images of relevant wafer areas with a) mc medium, b) HPM medium, c) HPM large, and d) HPM small at 70 % ingot height.

3.2 Lifetime and efficiency potential

To estimate the influence of the seed configurations on the material quality, minority charge carrier lifetime images at passivated wafer areas from the material with HPM large and HPM small seed plates were measured, see Figure 5a) and b). A higher square root harmonic mean lifetime of 330 µs is observable in HPM small compared to 210 µs in HPM large. This is due to the visible dislocation structures in the material with larger grains,

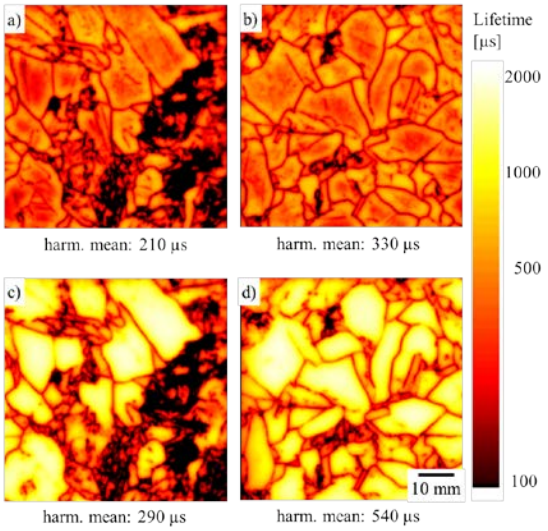

Figure 5: Minority charge carrier lifetime mappings at an illumination of 0.05 suns of relevant wafer areas at 70 % ingot height and corresponding harmonic mean values. Initial lifetimes at passivated samples of a) HPM large and b) HPM small and lifetimes at samples after boron diffusion of c) HPM large and d) HPM small. Note the logarithmic scaling.

As one process step towards the final solar cell, a boron diffusion has been applied. This process enables a

much higher lifetime in the grains compared with the as initial, of up to 2 ms for some larger grains, see Figure 5c) and d). Recombination active areas, grain boundaries and dislocations, are still visible. The harmonic mean lifetime was increased for both samples. The HPM large material reaches a mean lifetime of 290 µs, the HPM small material performs even better with 540 µs.

Based on injection-dependent lifetime images in combination with PC1D cell simulations, the efficiency potential for these materials combined with a high efficiency cell concept for n-type silicon was calculated via ELBA analyses. The used solar cell model features an efficiency limit without bulk recombination of 20.9 % for samples with an isotextured front surface [9]. The material nucleated on the finely grained HPM seed plates features higher efficiency potentials than the material nucleated on the larger grained HPM seed plate for all considered ingot heights, see Figure 6. The efficiency potential increases even for the highest ingot position, whereas the efficiency potential of the sample on HPM large stays constant.

In detail the material nucleated on the larger grained HPM seed features a global efficiency potential of 20.2 %, whereas the material nucleated on the finely grained HPM seed performs a global efficiency potential of 20.5 % on the relevant wafer area at 70 % ingot height. This means that only 0.4 % of the absolute efficiency is lost due to material-related recombination for the applied solar cell model with a cell limit of 20.9 %. The HPM small material is even slightly better than material nucleated on granular beads in a completely comparable process, providing an efficiency potential of 20.4 % at 70 % ingot height.

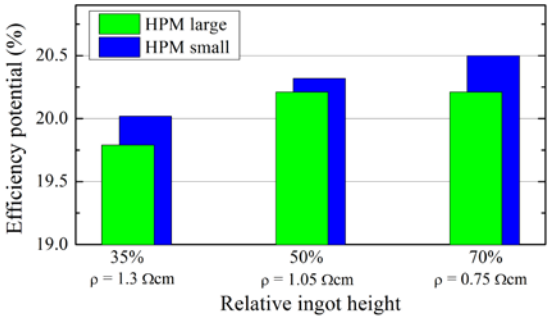

Figure 6: Efficiency potentials for the materials nucleated on HPM small and HPM large at three different ingot heights. The resistivities ρ at the considered ingot heights are noted below.

4 DISCUSSION

The saturation of the mean grain area as well as the described percentiles at the same ingot height for all HPM seeds as shown in Figures 1 and 2 suggest a dependence of the coarsening behavior on crystallization conditions, which were the same for both ingots. The growth velocity can be excluded as a possible reason because previous experiments with the same thermal conditions have shown a fairly constant growth velocity for the whole crystallization excepting bottom and top region. Furthermore, spatially resolved resistivity measurements at the brick side, not shown here, exhibit a flat and homogeneous form of the phase boundary at this height, which is relatively stable over a large part of the ingot height. This cannot explain the saturation of the grain coarsening. One possibility is that this effect is owed to the relative ingot height, i.e. the height of melt in front of the phase boundary influencing thermal conditions. Yet none of our previous experiments on G1 sized ingots have shown such saturation. This should be investigated in further experiments. A more probable factor is the crystallized ingot height, which would account for the different behavior for G1 sized ingots. The existence of an energetic minimum of the grain structure could lead to saturation in grain coarsening. Further experiments with higher ingots could cast more light on this relation.

The area share of twins increases for the HPM parts with ingot height and reaches a constant level. This trend can be explained by a growth model which proposes a grain elongation with ongoing growth [12]. Samples grown on the finer grained seed material, HPM small, start with a lower share of twins and end up at the same area share like the other samples, even the multicrystalline seed material, which is similar to results in the literature [8]. The grain structure of all different seed configurations develops to an area share of twins of between 15 % and 20 % at ingot top, which matches with reported experiments as well [3; 8].

The trend that smaller grains reduce dislocation structures faster and more efficient in the growth process, as illustrated by PL images, could be seen in the minority charge carrier lifetime images, as well. Even though the investigated material with larger grains is less limited by grain boundaries, the higher amount of dislocation structures reduces the harmonic mean lifetime in the initial state. The boron diffusion used for a high efficiency solar cell process intensifies this tendency. The gettering effect enhances the bulk lifetime inside the grains. Impurities concentrated at structural defects, grain boundaries and dislocations, are released into the bulk material due to the high temperature step and only partly gettered during the boron diffusion and in the subsequent cooling. Hence, regions with high initial lifetimes improve and regions with lower lifetimes deteriorate.

The material with smaller grains outperforms the larger grained material at all considered ingot heights. The improvement of the efficiency potentials from 35 % ingot height to 50 % ingot height is visible for both materials, HPM large and HPM small, and can be explained by the increase of the mean grain size, which reduces the area fraction of grain boundaries and thus recombination. Another factor for the increase of the efficiency potential is the decreasing resistivity as a lower resistivity has a positive effect on the efficiency potential for this cell concept in the range of the investigated lifetimes. The difference in the efficiency potential between the material nucleated on HPM small and HPM large can be entirely attributed to the crystal structure characteristics. This effect is most dominant for the highest ingot position, where the mean grain area of both seed configurations is comparable but the area fraction of dislocation structures is different. Hence, the benefit of the material nucleated on the HPM small seed is due to a lower dislocation density based on a different grain development showing that the dislocation density does not depend on the mean grain area only but on the evolution of the grain structure during crystallization.

At 70 % ingot height, he efficiency losses due to the material quality for the finely grained HPM seed plate are very low with 0.4 $\%_{abs}$. Therefore, the seed plate with

smaller grains seems to be the appropriate seed material for high efficiency solar cells.

Compared to previously crystallized HPM silicon with the same thermal conditions nucleated on granular silicon beads, the HPM small shows higher lifetimes as well [5]. Especially for the essential high temperature step, the wafer from the granular seed process features lifetimes of 350 µs harmonically averaged on the relevant wafer area at illumination of 0.05 suns compared to the wafer from the HPM small process with 540 µs. The use of seed plates with small HPM grain structure seems to be beneficial for higher efficiencies featuring a global efficiency potential of 20.5 %. There are two possible reasons for this effect. On the one side, the different geometry of the seed material, i.e. the difference between a completely solid seed plate and a loose granular structure, might have an influence. On the other side, the mean grain area of the investigated HPM small seed plate might be the optimum trade-off between larger grains to reduce recombination due to grain boundaries and grains small enough to guarantee a constantly low dislocation density to reduce recombination due to dislocations. This correlation was not further examined in this work and would require further experiments with seed plates.

5 CONCLUSION

A dependence of the coarsening of grains on the ingot height, probably determined by the already crystallized ingot height, was observed with saturation at about 150 mm ingot height. The mean grain area seems to affect the grain coarsening as well, showing a faster coarsening for smaller grain structures. The development of recombination active dislocation structures depends on this grain size and its distribution. The material nucleated on seed plates with HPM structure shows smaller areas affected by dislocations than that on the mc seed plate, as reported as benefit of HPM materials.

The HPM seed plate with the smallest initial grain size features the highest lifetimes in the initial and boron diffused state as well as the highest efficiency potential of 20.5 %. Lifetimes and efficiency potential are slightly higher compared to similarly crystallized HPM material with granular seeds.

6 ACKNOWLEDGEMENTS

The authors would like to thank Wacker Polysilicon for the silicon materials and express their gratitude to the crystallization, cell processing and characterization teams at ISE for their support and input in many valuable discussions. This work was funded by the German Federal Ministry for Economic Affairs and Energy within the research projects “THESSO” (grant number 0325491) and “multiTOP” (grant number 0324034).

7 REFERENCES

[1] A. Metz, et al., "International Technology Roadmap for Photovoltaic (ITRPV)", July 2015.

[2] G. Stokkan, Y. Hu, Ø. Mjøs, and M. Juel, "Study of evolution of dislocation clusters in high performance multicrystalline silicon", *Solar Energy Materials and Solar Cells* **130 (**2014) 679.

[3] Y. M. Yang, A. Yu, B. Hsu, W. C. Hsu, A. Yang, and C. W. Lan, "Development of high-performance multicrystalline silicon for photovoltaic industry", *Prog. Photovolt: Res. Appl.* **23 (**2015) 340.

[4] D. Zhu, L. Ming, M. Huang, Z. Zhang, and X. Huang, "Seed-assisted growth of high-quality multi-crystalline silicon in directional solidification", *Journal of Crystal Growth* **386 (**2014) 52.

[5] S. Riepe, P. Krenckel, F. Schindler, and C. Schmid, "Development of multicrystalline silicon for 20 % efficient n-type solar cells", *31st European Photovoltaic Solar Energy Conference and Exhibition (*2015).

[6] B. Michl, M. Kasemann, W. Warta, and M. C. Schubert, "Wafer thickness optimization for silicon solar cells of heterogeneous material quality", *Phys. Status Solidi RRL* **7 (**2013) 955.

[7] B. Michl, M. Rüdiger, J. A. Giesecke, M. Hermle, W. Warta, and M. C. Schubert, "Efficiency limiting bulk recombination in multicrystalline silicon solar cells", *Solar Energy Materials and Solar Cells* **98 (**2012) 441.

[8] T. Strauch, M. Demant, P. Krenckel, S. Riepe, and S. Rein, "Key Parameters for Brick Characterization of Grain Structure via Image Processing based on Optical Measurements of as-cut Si Wafers", *43rd IEEE Photovoltaic Specialist Conference (*2016).

[9] F. Schindler, et al., "High-Efficiency Multicrystalline Silicon Solar Cells: Potential of n-Type Doping", *IEEE J. Photovoltaics* **5 (**2015) 1571.

[10] J. A. Giesecke, M. C. Schubert, B. Michl, F. Schindler, and W. Warta, "Minority carrier lifetime imaging of silicon wafers calibrated by quasi-steady-state photoluminescence", *Solar Energy Materials and Solar Cells* **95 (**2011) 1011.

[11] F. Feldmann, M. Bivour, C. Reichel, H. Steinkemper, M. Hermle, and S. W. Glunz, "Tunnel oxide passivated contacts as an alternative to partial rear contacts", *Solar Energy Materials and Solar Cells* **131 (**2014) 46.

[12] R. R. Prakash, T. Sekiguchi, K. Jiptner, Y. Miyamura, J. Chen, H. Harada, and K. Kakimoto, "Grain growth of cast-multicrystalline silicon grown from small randomly oriented seed crystal", *Journal of Crystal Growth* **401 (**2014)